ROYAL SOCIETY
OF CHEMISTRY

PAPER

Flattening of multiwalled carbon nanotubes by electromigration-driven ductile deformation of Ni nanorod filler

Ren Yasuoka [ID] [a] and Hideo Kohno [ID] *[bc]

Ductile deformation and fracture of solid Ni nanorod fillers inside multiwalled carbon nanotubes were induced using the force induced by electromigration in a transmission electron microscope. The ductile elongation caused partial or full flattening of some host nanotubes, whereas other tubes remained cylindrical during the ductile process. The presence or absence of flattening of the host tubes was examined in terms of diameter, wall thickness, and magnitude of electric current.

1 Introduction

Carbon nanotubes[1,2] (CNTs) exhibit excellent properties. In addition to electronic and optic applications,[3–6] CNTs can be used as various sensors.[7–10] CNTs also exhibit excellent mechanical properties and have therefore been used to reinforce various materials.[11] In addition to such passive mechanical functionalities of CNTs, active mechanical functionalities would broaden the range of applications of CNTs. Electromigration-driven actions of nanomaterials inside CNTs are promising for manipulating the shape of CNTs. In our previous paper,[12] electromigration-driven motion of Co nanorods inside multiwalled CNTs (MWCNTs) was used to unflatten the host MWCNTs; however, electromigration motion of nanoscale objects inside CNTs has not enabled the controlled flattening of CNTs.

Ductile deformation is a promising approach to realize the flattening of CNTs using electromigration-driven action of nanoscale objects inside CNTs. Transmission electron microscopy (TEM) observations of ductile deformation of nanocontacts of various metals have been performed using micromanipulator systems, in which nanocontacts were manipulated by the mechanical motion of the micromanipulators.[13–19] In the present study, ductile deformation of Ni nanorod fillers was induced in MWCNTs using the force of electromigration. The associated deformations of the host MWCNTs was also investigated.

2 Experimental

Ni-filled MWCNTs were fabricated as follows. A 30 nm-thick Ni layer was deposited onto a polycrystalline Al_2O_3 substrate. The substrate was sealed in an evacuated silica tube with 3 mg of a mixture of graphite, hexadecanoic acid [$CH_3(CH_2)_{14}COOH$], and saccharin [$C_7H_5NO_3S$] at a weight ratio of 664 : 86 : 1. The sample was heated to 1100 °C for 20 min for the growth of Ni-filled MWCNTs. TEM observations of such Ni-filled MWCNTs are described in our previous work.[20] The Ni-filled MWCNTs were mounted onto a Au wire, which functioned as a ground electrode. The Au wire with Ni-filled MWCNTs was mounted on a micromanipulator TEM sample holder (Kitano Seiki). A W needle was used as a bias electrode. *In situ* TEM observations were carried out using a TEM (JEM-ARM200F, JEOL) operated at 200 kV. Movies of TEM observations were recorded at 25 frames per second (fps) using a camera (Rio16, Gatan) with a resolution of 1024 × 1024 pixels. A source-measure unit (GS610, Yokogawa) was used to apply and measure the electric current.

3 Results and discussion

Fig. 1(a) shows the experimental setup for TEM observations of ductile deformations of Ni nanorod fillers inside MWCNTs. A MWCNT with a Ni nanorod filler is mounted on a grounded Au wire, and a biased W needle is located in the middle of the Ni filler. An electric current is applied between the Au and W electrodes, and the right portion of the Ni filler between the electrodes is pulled to the right along the direction of the flow of electrons by the force of electromigration, while the force of electromigration does not work on the left portion of the Ni nanorod filler. When the left portion of the Ni filler is long enough, the left portion does not move to the right due to the friction, while the right portion moves to the right due to the force of electromigration resulting in the ductile deformation of the Ni nanorod filler around the contact between the sample

[a]School of Environmental Science and Engineering, Kochi University of Technology, Kami, Kochi 782-8502, Japan

[b]School of Engineering Science, Kochi University of Technology, Kami, Kochi 782-8502, Japan. E-mail: kohno.hideo@kochi-tech.ac.jp; Tel: +81 887-57-2506

[c]Carbon Neutral Functional Materials Research Center, Kochi University of Technology, Kami, Kochi 782-8502, Japan
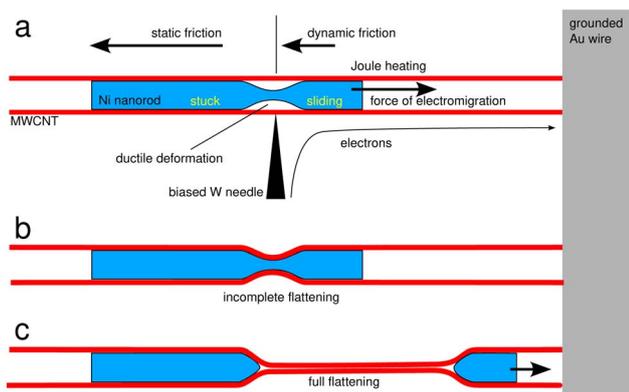
Fig. 1 Schematic illustration of the experimental setup, and expected processes: (a) without MWCNT's deformation, (b) with an incomplete flattening, and (c) with a full flattening of the MWCNT.

and the W needle. Fig. 1(a) also represents the case where deformation of the MWCNT does not occur. Fig. 1(b) and (c) represent the cases where an incomplete or a full flattening of the MWCNT occurs, respectively.

When an electric current was applied to a MWCNT with a Ni nanorod filler, ductile deformation and fracture of the Ni nanorod filler occurred as shown in Fig. 2 (SI Movie SM1). The Ni nanorod filler was 32 nm thick, and the magnitude of the applied electric current was 50 μA. Electrons flowed in the Ni nanorod filler rightward from the point of contact with the W needle; the force due to electromigration therefore acted only on the right portion of the Ni nanorod filler [Fig. 2(a)]. The left portion of the Ni filler was subject only to the force of friction. First, ductile elongation occurred at the middle portion of the filler [Fig. 2(b)], forming an empty space inside the MWCNT; the elongation then increased [Fig. 2(c)] until the thin portion became segmented [Fig. 2(d and e)]. Subsequently, the divided elongated portions moved back to each segment because of surface tension and then disappeared. In this first demonstration, we did not observe substantial deformation of the host MWCNT.

During the ductile deformation process, the Ni nanorod filler showed clear diffraction contrast; therefore, the filler was solid and the deformation was plastic. The filler and its host MWCNT were Joule-heated, and the temperature was below the melting point of Ni during the ductile process. The forces due to electromigration and friction were considered to be approximately 10^{-24} N according to our previous studies.[12,21] Therefore, this force is sufficient to cause ductile plastic deformation of the Ni nanorod.

As shown in Fig. 1, the force of electromigration F_e and the sliding friction F_f worked on the sliding right portion of the Ni nanorod filler. The total force, F_e-F_f, pulled the right portion causing the ductile deformation. The strength of the maximum static friction working on the left portion must have been larger than the total force worked on the right portion. From the measured values of the strengths of the force of electromigration and the sliding friction in our previous study,[21] the total force worked on the right portion of the Ni nanorod filler is
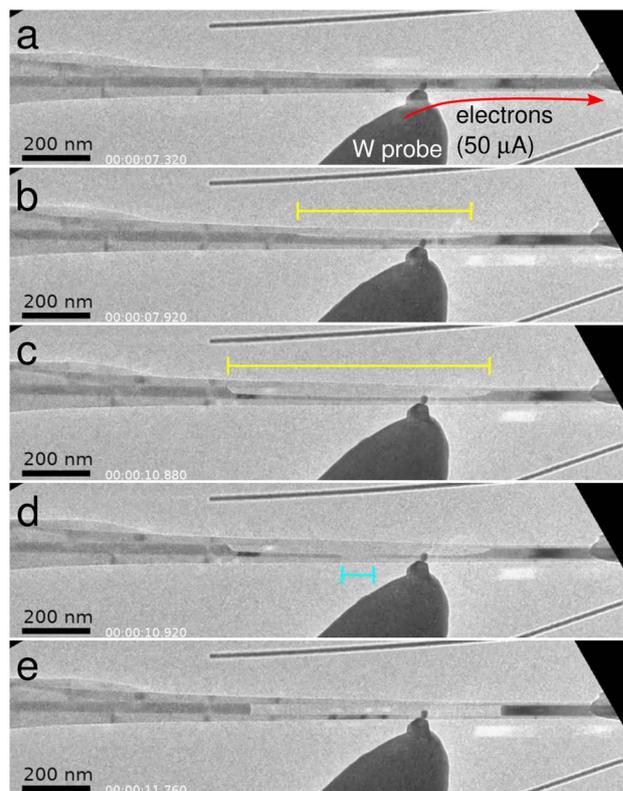

Fig. 2 *In situ* TEM observations of electromigration-induced ductile deformation of Ni nanorod filler inside MWCNT. (a) A 50 μA flow of electrons was induced in the right portion of a Ni-filled MWCNT, forcing this portion to the right. (b) Ductile deformation of the filler occurred at the region marked by the yellow bar, forming an empty space inside the MWCNT, and (c) the ductile deformation region became longer. (d) The Ni nanorod filler was segmented at the region marked by the blue bar, and the thin ductile-deformed portions remained. (e) The thin ductile-deformed portions were pulled into the thick portions of the segments because of surface tension (SI Movie SM1 available).

estimated to be around $10^{-25}-10^{-24}$ [N]. Using this value and the diameter of the Ni nanorod filler, the strength of the tensile stress is estimated to be around $10^{-16}-10^{-15}$ [N mm^{-2}]. This value is much smaller than known values of yield stress of bulk polycrystalline Ni, *ca.* 100–500 [N mm^{-2}].[22] We speculate that the Ni nanorod filler was Joule-heated at around 1.3×10^3 [K] according to our previous studies,[21,23] and the Joule heating softened the Ni nanorod filler. It is also likely that the size effect also caused the softening because the melting points of nanomaterials becomes lower.[24,25] It should also be noted that the observed ductile deformation would have been related to superplasticity.[26]

In another demonstration, we observed partial flattening of a host MWCNT during electromigration-induced elongation of a Ni nanorod filler [Fig. 3 (SI Movie SM2)]. As shown in Fig. 3(a), a W probe was connected to the MWCNT at the middle position of the Ni nanorod filler, and an electric current of 150 μA was applied. The left portion of the Ni nanorod filler was forced along the direction of electron flow (*i.e.*, to the left). The filler
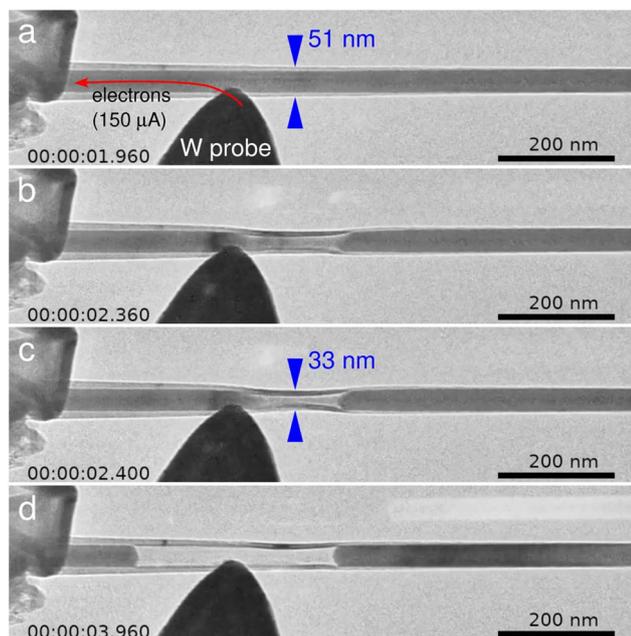
Fig. 3 *In situ* TEM observation of electromigration-induced ductile deformation of Ni nanorod filler inside MWCNT, accompanied by partial flattening of host MWCNT. (a) A 150 μA flow of electrons was induced in the left portion of a Ni-filled MWCNT, forcing this portion to the left. (b) The middle portion of the filler became elongated and thin near the point of electric contact, and the host MWCNT partially flattened at the portion where the filler was elongated. (c) The elongation and the flattening became more obvious. (d) The filler segmented, and the partial flattening of the MWCNT almost recovered (SI Movie SM2 available).

became elongated near the point of electric contact with the W needle, and the host MWCNT partially flattened at the region of elongation, without creating an empty space between the filler and the MWCNT; the width of the MWCNT decreased from 51 nm to 33 nm [Fig. 3(b and c)]. Finally, the filler was segmented at the elongated portion and the partial flattening of the MWCNT recovered [Fig. 3(d)]. After segmentation of the filler, the edges of the newly formed nanorod became rounded because of surface tension; empty space was then formed between the two divided portions.

The filler showed clear image contrast that originated from Bragg diffraction, indicating that, as in the first demonstration, the filler remained solid. The lack of empty space during the processes of elongation and partial flattening is evidence that the flattening was caused by hydrophilic contact between the filler and the MWCNT; specifically, the elongating filler pulled the sidewall of the MWCNT inward.

Fig. 4 (SI Movie SM3) shows a third demonstration, in which flattening of a host MWCNT was full and stable. In this example, the magnitude of the applied electric current was 110 μA and the Ni nanorod filler was solid, as observed in the other demonstrations [Fig. 4(a)]. First, the filler became thinner at the contact position and the MWCNT partially flattened at that position, without forming an empty space between the filler and the MWCNT [Fig. 4(b)]. The filler then segmented near the point
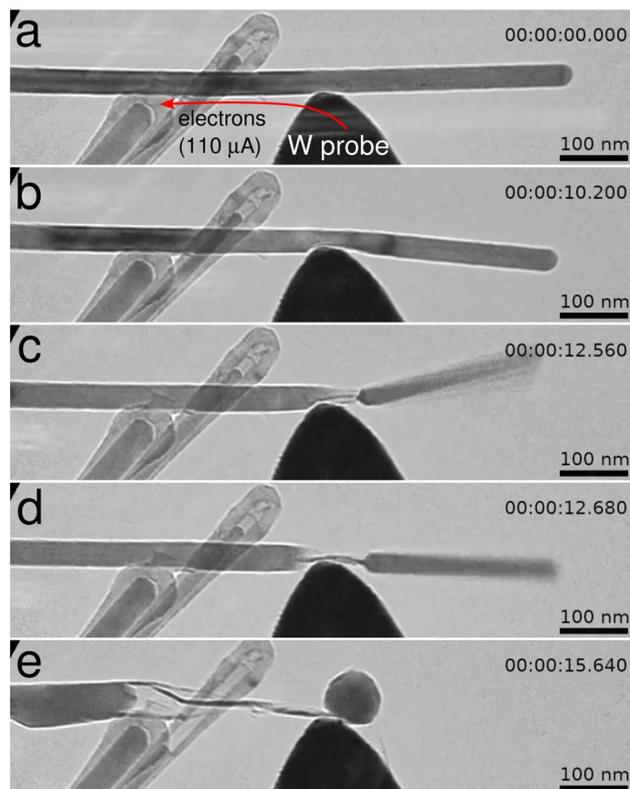

Fig. 4 *In situ* TEM observations of electromigration-induced ductile deformation of Ni nanorod filler inside MWCNT, accompanied by full flattening of MWCNT. (a) A 110 μA flow of electrons was induced in the left portion of a Ni-filled MWCNT, forcing the left portion of the filler to the left. (b) The filler became thin at the point of contact, and the MWCNT partially flattened. (c) The thinning proceeded further and the filler was divided; the MWCNT fully collapsed at the position of the division of the filler. (d) The left portion of the filler moved leftward, and the flattened portion of the MWCNT became longer. (e) Flattening of the MWCNT proceeded as the filler moved farther to the left (SI Movie SM3 available).

of contact with the W needle electrode, whereas the MWCNT flattened fully near the contact position [Fig. 4(c)]. After the segmentation of the filler, the left portion moved leftward under the electromigration force and the flattened portion became longer [Fig. 4(d)]. Flattening of the MWCNT proceeded as the filler moved farther to the left [Fig. 4(e)].

The fourth demonstration shows a two-step flattening of a MWCNT as a result of ductile elongation of a Ni nanorod filler [Fig. 5 (SI Movie SM4)]. The right portion of the filler was forced rightward by a 100 μA flow of electrons [Fig. 5(a)]. First, the left portion of the filler became elongated, forming an empty space at the bottom half of the MWCNT [Fig. 5(b)]. At this stage, the bottom portions of the sidewall adjoining the empty space, especially the inner edge of the bottom sidewall (indicated by the arrowhead) showed clear image contrast, indicating that this portion of the MWCNT remained cylindrical. The image of the inner edge of the bottom sidewall of the MWCNT at this portion became unclear [Fig. 5(c)]; we therefore judged that the bottom half of the MWCNT at this portion became flattened
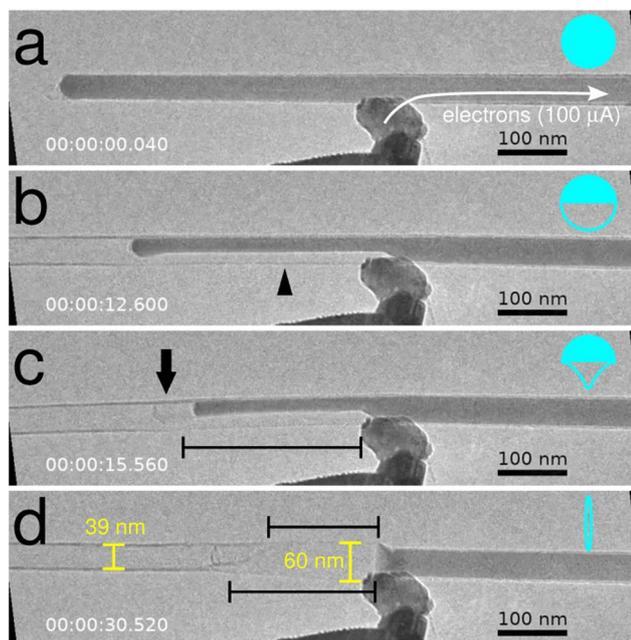
Fig. 5 Two-step flattening of MWCNT caused by electromigration-driven ductile elongation of Ni nanorod filler. (a) Before the elongation of the filler. (b) The left portion of the filler elongated inside the cylindrical tube. (c) The bottom half of the tube flattened below the elongated filler at the portion indicated by the bar. (d) The middle portion of the tube fully flattened (see the portion indicated by the bars); the left end of the filler became wedge-shaped because of the nanotube flattening. The blue marks at the right corners of the TEM micrographs illustrate proposed cross-sectional structures near the position indicated by the arrowhead (SI Movie SM4 available).
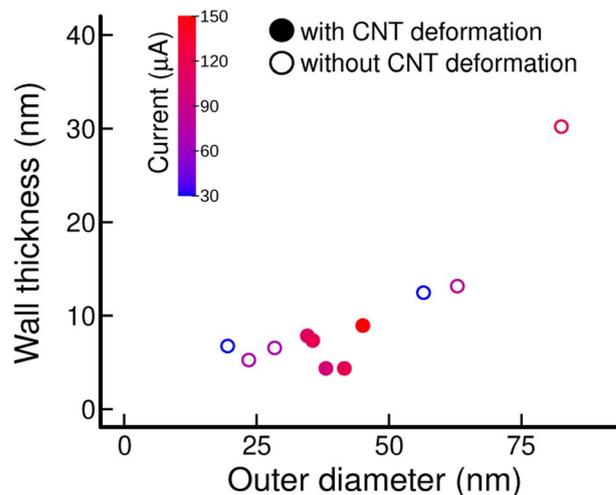

Fig. 6 Plot indicating the presence or absence of flattening of the host MWCNTs in terms of the MWCNT diameter and wall thickness and the magnitude of the applied electric current.

along the viewing direction. We also note that a short MWCNT was formed at the left tip of the elongated filler, as indicated by the arrow. Finally, the left elongated portion was forced rightward and vanished around the point of electric contact with the biased probe electrode. At this stage, both the top and bottom of the MWCNT sidewall became unclear, showing that the portion near the contact was fully flattened along the viewing direction. The image contrast of the left edge of the Ni nanorod filler at the contact showed gradation: the image contrast became increasingly pale toward the left edge; thus, the left edge of the filler became tapered. The wedge shape of the left edge of the filler matches the flattening of the MWCNT. The MWCNT was 60 nm wide near the left edge of the filler, whereas the MWCNT was 39 nm at the cylindrical portion. When a very thin cylinder becomes fully flattened, its width becomes larger by a factor of $\pi/2 \simeq 1.57$; the observed widening factor was approximately 1.5. This difference is also evidence of full flattening of the portion of the MWCNT near the contact.

When a Ni nanorod filler was elongated because of ductile deformation driven by the electromigration force, some host MWCNTs showed marked flattening, whereas others did not. Flattening of CNTs has been well studied,[27–37] and the flattening behavior is known to depend on a CNT diameter and wall number. CNTs with a larger diameter and a thinner sidewall tend to be flattened. In the present study, Joule heating would

have affected the flattening behavior of the host MWCNTs. Fig. 6 shows a plot of data indicating whether deformation—specifically, flattening—occurred on the basis of the outer diameter and wall thickness of the MWCNTs and the magnitude of the electric current. We used the magnitude of the electric current for two reasons: we could not use current density because the cross-sectional area of a Ni nanorod filler changes during the electromigration process, and a reliable estimation of the sample temperature was not possible. Fig. 6 shows that, to cause flattening of a host MWCNT, its sidewall should be thinner than approximately 10 nm and its outer diameter should be approximately 30–50 nm. In addition, an electric current greater than 100 µA is required. For the three samples with a very small diameter, their sidewalls were as thick as MWCNTs with an outer diameter between 30 and 50 nm; therefore, the three MWCNTs should have been harder than the MWCNTs that showed flattening.

4 Conclusions

Ductile deformation and fracture of Ni nanorod fillers inside MWCNTs were induced using the forces due to electromigration and friction. In some cases, these effects induced partial or full flattening of the host MWCNTs. In addition, the MWCNT diameter and sidewall thickness and the magnitude of the electric current required to induce flattening of MWCNTs were revealed.

The ductile deformations of Ni nanorod fillers inside MWCNTs would be useful for studying plastic and elastic deformations of and defect formations in deformed nearly-free-standing nanomaterials with a well-defined, restricted outer diameter and shape. The flattening of MWCNTs caused by the ductile deformation of the Ni nanorod fillers would be useful to close the inner paths of MWCNTs when the MWCNTs are used to transport nano-objects inside them. It is also expected that the caused flattening of the MWCNTs changes local electronic

properties and surface chemical activities of the MWCNTs at the flattened portions. When MWCNTs are used as a reinforcing material, the junctions of cylindrical and flattened portions would work as anchors against sliding of the MWCNTs in the host material. The flattening of MWCNTs caused by the ductile deformation of Ni nanorod fillers would also be useful for microelectromechanical system (MEMS) and nano-electromechanical systems (NEMS).

Conflicts of interest

There are no conflicts to declare.

Data availability

The data supporting this article have been included as part of the supplementary information (SI). Supplementary information: Movie SM1–4. See DOI: https://doi.org/10.1039/d5na01118c.

References

1 S. Iijima, *Nature*, 1991, **354**, 56–58.

2 S. Iijima and T. Ichihashi, *Nature*, 1993, **363**, 603–605.

3 R. Maheswaran and B. P. Shanmugavel, *J. Electron. Mater.*, 2022, **51**, 2786–2800.

4 X. Wei, S. Li, W. Wang, X. Zhang, W. Zhou, S. Xie and H. Liu, *Adv. Sci.*, 2022, **9**, 2200054.

5 A. D. Franklin, M. C. Hersam and H.-S. P. Wong, *Science*, 2022, **378**, 726–732.

6 J. Zaumseil, *Adv. Opt. Mater.*, 2022, **10**, 2101576.

7 A. Hendler-Neumark, V. Wulf and G. Bisker, *ACS Sens.*, 2023, **8**, 3713–3722.

8 K. Boonyaves, M. C.-Y. Ang, M. Park, J. Cui, D. T. Khong, G. P. Singh, V. B. Koman, X. Gong, T. K. Porter, S. W. Choi, *et al.*, *Nano Lett.*, 2023, **23**, 916–924.

9 R. Wang, L. Sun, X. Zhu, W. Ge, H. Li, Z. Li, H. Zhang, Y. Huang, Z. Li, Y.-F. Zhang, *et al.*, *Adv. Mater. Technol.*, 2023, **8**, 2200855.

10 H. Zhao, J. Han, M. Zhao, Z. Hui, Z. Li and S. Komarneni, *Food Chem.*, 2025, **472**, 142993.

11 S. R. Bakshi, D. Lahiri and A. Agarwal, *Int. Mater. Rev.*, 2010, **55**, 41–64.

12 S. Kato, S. Matsuyama and H. Kohno, *J. Phys. Soc. Jpn.*, 2024, **93**, 124601.

13 T. Matsuda and T. Kizuka, *Jpn. J. Appl. Phys.*, 2009, **48**, 115003.

14 K. Ishizuka, M. Tomitori, T. Arai and Y. Oshima, *Appl. Phys. Express*, 2020, **13**, 025001.

15 T. Kizuka, *Phys. Rev. B:Condens. Matter Mater. Phys.*, 1998, **57**, 11158.

16 K. Yamada and T. Kizuka, *Sci. Rep.*, 2017, **7**, 42901.

17 Y. Oshima and Y. Kurui, *Phys. Rev. B:Condens. Matter Mater. Phys.*, 2013, **87**, 081404.

18 T. Ishida, T. Sato, S. Nabeya, K. Kakushima and H. Fujita, *Jpn. J. Appl. Phys.*, 2011, **50**, 077201.

19 J. Zhang, M. Tomitori, T. Arai and Y. Oshima, *Phys. Rev. Lett.*, 2022, **128**, 146101.

20 K. Nakaoka and H. Kohno, Submitted.

21 K. Adachi, S. Matsuyama, Y. Sakai and H. Kohno, *Nanoscale Adv.*, 2024, **6**, 1480–1485.

22 Y. Zhao, T. Topping, J. F. Bingert, J. J. Thornton, A. M. Dangelewicz, Y. Li, W. Liu, Y. Zhu, Y. Zhou and E. J. Lavernia, *Adv. Mater.*, 2008, **20**, 3028–3033.

23 S. Ohba and H. Kohno, *J. Phys. Soc. Jpn.*, 2022, **91**, 123601.

24 E. Roduner, *Chem. Soc. Rev.*, 2006, **35**, 583–592.

25 S. Srivastava, A. K. Pandey and C. K. Dixit, *Natl. Acad. Sci. Lett.*, 2025, **48**, 123–127.

26 G. Cao, J. Wang, K. Du, X. Wang, J. Li, Z. Zhang and S. X. Mao, *Adv. Funct. Mater.*, 2018, **28**, 1805258.

27 D. Choi, Q. Wang, Y. Azuma, Y. Majima, J. Warner, Y. Miyata, H. Shinohara and R. Kitaura, *Sci. Rep.*, 2013, **3**, 1617.

28 S. Liu, J. Yue and R. J. Wehmschulte, *Nano Lett.*, 2002, **2**, 1439–1442.

29 W. Li, X. Yan, K. Kempa, Z. Ren and M. Giersig, *Carbon*, 2007, **45**, 2938–2945.

30 M. S. Mazzoni and H. Chacham, *Appl. Phys. Lett.*, 2000, **76**, 1561–1563.

31 M. Minary-Jolandan and M.-F. Yu, *J. Appl. Phys.*, 2008, **103**, 073516.

32 N. G. Chopra, L. X. Benedict, V. H. Crespi, M. L. Cohen, S. G. Louie and A. Zettl, *Nature*, 1995, **377**, 135–138.

33 E. Picheau, A. Impellizzeri, D. Rybkovskiy, M. Bayle, J.-Y. Mevellec, F. Hof, H. Saadaoui, L. Noé, A. C. Torres Dias, J.-L. Duvail, *et al.*, *ACS Nano*, 2021, **15**, 596–603.

34 J. Xiao, B. Liu, Y. Huang, J. Zuo, K. Hwang and M. Yu, *Nanotechnology*, 2007, **18**, 395703.

35 Y. Magnin, F. Rondepierre, W. Cui, D. Dunstan and A. San-Miguel, *Carbon*, 2021, **178**, 552–562.

36 V. Perebeinos and J. Tersoff, *Nano Lett.*, 2014, **14**, 4376–4380.

37 H. Kohno, T. Komine, T. Hasegawa, H. Niioka and S. Ichikawa, *Nanoscale*, 2013, **5**, 570–573.